Journal of King Saud University – Science 32 (2020) 2969–2975

Contents lists available at ScienceDirect

Journal of King Saud University – Science

journal homepage: www.sciencedirect.com

Original article

Characterization and potential applications of different powder volcanic ash

Shoroog Alraddadi [a,*], Hasan Assaedi [b]

[a] Department of Physics, Umm Al-Qura University, Makkah 24382, Saudi Arabia
[b] Department of Physics, University College in AlJumum, Umm Al-Qura University, Makkah 21955, Saudi Arabia

ARTICLE INFO

Article history:
Received 16 April 2020
Revised 27 July 2020
Accepted 30 July 2020
Available online 6 August 2020

Keywords:
Volcanic ash
Scoria
Pumice
Chemical composition
Morphological analysis
Environmental care

ABSTRACT

Objectives: In this study, the crystalline phase, microstructure, chemical composition, and morphology of the powder of volcanic ashes from three different places have been investigated.
Methods: The raw materials were initially milled and the particle size was decreased to approximately 74 μm. X-ray diffraction (XRD), chemical analysis (XRF and ICP-OES technique), Fourier transform infrared spectroscopy and scanning electron microscopy were used to examine the obtained samples.
Results: It was found that the volcanic ashes exhibit clear variations in mineralogy, chemical compositions, stretching vibrational modes, and morphological structure. All the samples have an amorphous phase and contain SiO_2, Al_2O_3, CaO, and Fe_2O_3 as their major constituents. Other oxides such as K_2O, MgO, MnO, Na_2O, P_2O_5, TiO_2, and SO_3 were found in minor percentages. The morphology of the samples showed a variety of volcanic mixtures with irregular shapes.
Conclusions: The abundant volcanic ash can be used as a new low-cost natural material in several applications such as in construction materials, ceramic industry, water purification, geopolymers, and other advanced technologies.

1. Introduction

Significant reserves of volcanic ashes are hosted by Saudi Arabia, primarily in the western region. They are considered as pyroclastic materials and their mineralogy as well as chemical compositions are associated with the magma from which they erupted. The obtained properties play an important role for the effective utilization of volcanic ash in various applications. However, the full potential of volcanic ashes is yet to be employed. The most important components for application purposes present in volcanic ash are in the form of scoria and pumice (Alemayehu and Lennartz, 2010; Best, 2013). These mixtures are rich and natural aluminosilicate geo-resources. They impart interesting physical properties and can range in sizes from sub-millimetric particles all the way up to sizes comparable to rocks (Brown and Calder, 2005).

The various applications of volcanic ashes such as in cement and concrete, geopolymer, ceramic, adsorbents, and lunar soil stimulants have been addressed in literature (Assaad et al., 2020; Liu and Taylor, 2011; Zheng et al., 2009; Wang et al., 2017; Lemougna et al., 2018, 2020). However, in comparison to the fly ash that has been subjected to extensive research (Ahmaruzzaman, 2010; Cultrone and Sebastián, 2009; Kumar et al., 2007; Toniolo and Boccaccini, 2017; Xu and Shi, 2018; Zhuang et al., 2016), insignificant work has been reported on volcanic ashes; this is despite the fact that they exhibit promising applications and can be easily procured from several unexploited deposits in many parts of the world (Alemayehu and Lennartz, 2009; Al-Fadala et al., 2017; Lemougna et al., 2011; Zheng et al., 2009). Due to their porosity, the mixture of scoria and pumice is easier to develop and thus would be attractive for industrial products (Alemayehu and Lennartz, 2009). The origin of the magma plays a key role in the composition and characteristics of the volcanic ash (Siddique, 2011). Many volcanic ashes exhibit a wide spectrum of SiO_2, Al_2O_3, CaO, Fe_2O_3, MgO, K_2O, and Na_2O as dominant components. Other oxides may also be found in lower proportions.

Generally, a large percentage of silica is present, as it is one of the largest oxides in the Earth's crust. Silica is found between 40

* Corresponding author.
E-mail address: swraddadi@uqu.edu.sa (S. Alraddadi).
Peer review under responsibility of King Saud University.

Production and hosting by Elsevier

https://doi.org/10.1016/j.jksus.2020.07.019
1018-3647/

Fig. 1. Raw (on the bottom) and powder (on the top) volcanic ash of the selected samples S3 (poor red color), S7 (white color), and S10 (black color).

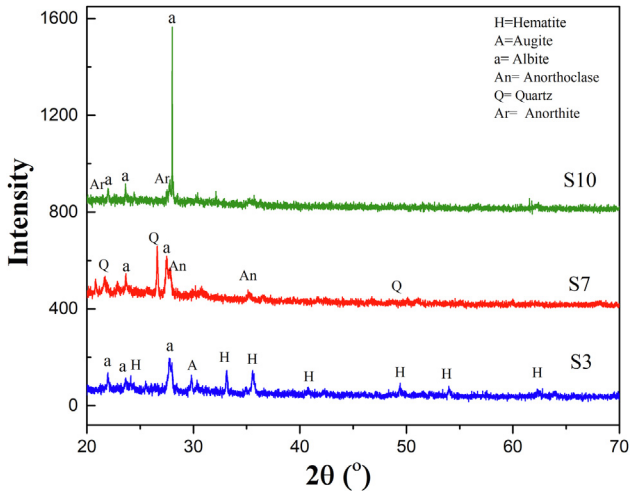

Fig. 2. XRD pattern of powder volcanic ash S3, S7, and S10.

and 52 wt% and 63–75 wt% in scoria and pumice, respectively (Lemougna et al., 2011; Siddique, 2011; Demirdag and Gunduz, 2008; Hossain, 2005; Leonelli et al., 2007; Kani, et al., 2012; Ohba and Nakagawa, 2002; Rocher, 1992; Seyfi et al., 2015; Takeda et al., 2014; Tchakoute et al., 2013). It is found that the volcanic ashes contain minerals originating from magma. The mineralogical composition of these minerals depends on both, eruption conditions and the magma configuration. The magma can have a nearly amorphous phase or completely crystalline structures (Lemougna et al., 2011, 2014; Nakagawa and Ohba, 2002; Serra et al., 2015; Zhang et al., 2017). The scoria form has colors ranging from black to poorly red and the pumice form has colors from black to white, having a porous or vesicular structure (Paulick and Franz, 1997; Alemayehu and Lennartz, 2009). The desirable application of the volcanic ash depends on the amount of amorphous phase, mineralogy, specific surface area, chemical composition, and particle size distribution (Koshino, 2001; Langmann et al., 2010; Querol et al., 2001; Kaid et al., 2009). The nature of Strombolian eruption resulted in the production of numerous cone-shaped scoria within the fields of basaltic lava found in the western area of Saudi Arabia. These fields are known as Harrats. Although volcanic ash deposits are abundant in these areas, little related work has been done in

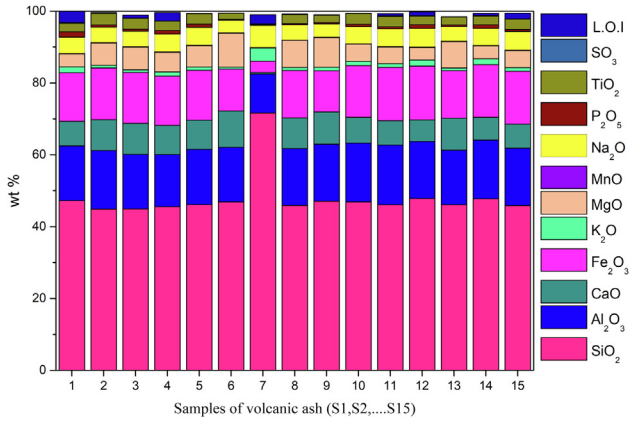

Fig. 3. Major and minor elements in the powder of all volcanic ashes by XRF (expressed as wt. % oxides).

Table1
Bulk density obtained by Ultrapycnometer.

Sample	S3	S5	S6	S7	S9	S10	S12	S15
Bulk density (g/cc)	3.30	3.10	3.16	2.73	3.02	3.13	3.17	3.061

Table 2
Chemical composition of the different volcanic ashes from previous study and suggested applications for comparison.

Elements	SiO_2	Al_2O_3	CaO	MgO	Fe_2O_3	Na_2O	K_2O	TiO_2	P_2O_5	MnO	SO_3	Potential applications
Our samples	44.8–71.6	10.8–16.64	0.42–8.94	3.57–9.47	3.14–14.70	3.45–6.1	0.58–3.62	0.15–3.23	0.22–1.46	0.07–0.42	0.25–0.04	–
Leonelli et al., 2007	44–47	14–16	8–10	3–7	10–14	3–4	1–3	2–4	0–0.7	0–0.5	–	Ceramics
Serra et al., 2015	70.43	15.03	1.45	0.64	3.52	5.43	2.76	0.5	–	–	–	Ceramics
Kaid et al., 2009	43–72	9–20	1–15.	0.5–7	1–12	0.5–11	0.2–8	–	–	–	–	Cement and Concretes
Lemougna et al., 2014	43–55	15–16	6–11	3–7	8–14	4.1–5.3	1.5–3	1.8-3.3	0.8–0.9	0.16-0.2	–	Geopolymers
Alemayehu and Lennartz, 2009	47.4-68.6	8.9-21.6	1.8-12.4	0.2-3.3	1.8-8.9	3.0-4.1	0.5-5.5	1.7-0.3	–	–	–	Absorbents for Cd
Zheng et al., 2009	49.24	15.8	7.25	8.72	11.47	3.08	1.03	1.91	0.3	0.14	20-40	Lunar soil simulant

Table 3
Trace elements for different samples collected from Harrat Rahat (S1, S5), Harrat Khaybar (S7, S9), and Harrat Lunayyir (S10, S15) (expressed in ppm by ICP–OES).

Elements	S_3	S_7	S_9	S_{10}	S_{15}
Ag	<1	<1	<1	<1	<1
As	<5.5	<5.5	<5.5	<5.5	<5.5
Ba	75.20	11.81	134.77	208.18	309.29
Be	1.69	24.34	1.33	1.67	2.09
Bi	<10	<10	<10	<10	<10
Cd	<0.5	<0.5	<0.5	<0.5	<0.5
Ce	34.58	224.32	35.05	55.08	83.28
Co	39.52	<1	36.70	32.27	24.67
Cr	88.93	16.14	237.37	18.27	124.40
Cu	45.85	1.88	54.99	30.26	25.21
Dy	3.83	28.62	3.03	5.14	7.54
Er	7.90	12.19	4.96	7.59	7.72
Eu	<1	<1	<1	<1	<1
Ga	<1	42.91	<1	<1	<1
Gd	6.00	24.75	4.33	8.13	10.06
Ge	<1	<1	<1	<1	<1
Hf	1.82	50.63	2.02	2.94	5.06
Ho	<1	5.86	<1	<1	<1
La	17.09	103.98	19.27	26.52	38.09
Li	5.33	108.39	5.81	7.18	11.83
Lu	1.48	2.75	1.15	1.41	1.80
Mo	<2	2.42	2.35	2.83	14.59
Nb	17.97	222.97	28.05	32.47	38.01
Nd	20.69	86.29	17.53	27.44	41.27
Ni	58.35	1.74	126.94	19.38	12.67
Pb	6.04	44.69	7.10	7.05	9.08
Pr	<5	25.83	<5	5.32	8.64
Rb	27.57	215.51	35.38	35.97	102.51
Sb	<10	<10	<10	<10	<10
Sc	21.70	<1	20.34	16.74	14.75
Sm	1.12	22.70	1.81	3.43	7.33
Sn	<10	24.55	<10	<10	<10
Sr	484.22	21.47	474.94	469.94	459.03
Ta	<1	19.37	<1	<1	<1
Tb	<1	6.11	<1	<1	<1
Th	<10	37.37	<10	<10	<10
Tm	<1	2.02	<1	<1	<1
U	<10	12.30	<10	<10	<10
V	260.03	6.04	184.92	177.60	76.03
W	<5	<5	<5	<5	<5
Y	23.01	194.39	17.25	31.84	46.02
Yb	3.10	20.60	2.28	4.09	5.28
Zn	94.28	304.96	110.06	106.74	122.09
Zr	209.67	2302.89	186.50	276.95	402.30

utilizing its properties as a light-weight aggregate, which can be used in building materials for construction and insulating purposes. Hence, there is a dire need for innovative methods of preparation of smarter materials for applications in high-tech products and raw materials for advanced technologies such as packaging, sensors, additives, catalysis and polymer networks. Consequently, certain applications of volcanic ash will lead to strategic and economic trends.

The aim of this work is to explore the physicochemical properties of different volcanic ash samples collected from three different places and suggest their potential applications. To the best of our knowledge, such a study was never performed before on these materials. The western region of the Kingdom of Saudi Arabia has large reserves of natural volcanic ash (pozzolan) covering an estimated area of 180,000 km^2 (Sabtan and Shehata, 2000). The phase and mineralogical characterization of the ashes was achieved using X-ray diffraction (XRD), while the functional groups of chemical contents were obtained by using Fourier transform infrared spectroscopy (FTIR). Further, the chemical composition was analyzed using X-ray fluorescence spectrometry (XRF), major trace element detection and measurements were performed by employing the inductively coupled plasma (ICP) technique and morphological analysis was accomplished by scanning electron microscopy (SEM).

2. Materials and methods

Fifteen samples of volcanic ash were collected from three separate areas of Saudi Arabia including: Harrat Rahat (S1, S2, S3, S4, S5), Harrat Khaybar (S6, S7, S8, S9) and Harrat Lunayyir (S10, S11, S12, S13, S14, S15). The raw materials of the volcanic ashes with particle sizes between 0.01 and 0.32 mm and different colors such as black, poor red, and white are shown in Fig. 1. All the samples were ground by ball milling to obtain approximately 74 μm sized homogeneous powders which were then sieved through 200 meshes to remove unwanted particles. Samples were selected based on their physical appearance and chemical composition to be further examined by XRD and FTIR. The samples (S3, S7, and S10) were subjected to further measurements as they vary greatly in both their appearance and chemical composition, while similar samples were excluded. The crystalline phase composition and mineralogy were carried out using XRD (Philips PW 1710 diffract-meter, equipped with Cu K and Ni-filter radiation). The samples were scanned from 5° to 75°. The sample's bulk density was evaluated using Ultrapycnometer 1000. The FTIR characterization of the raw and powder samples was done using Nicolet (iS50 FTIR), and recorded over the range of 4000–400 cm^{-1} at room temperature. The chemical compositions of the ashes were determined using X-ray fluorescence (XRF) for major and minor elements

(SPECTRO – EXPOS) and inductively coupled plasma mass spectrometry (ICP-OES) (Optical Emission Spectrometer – Optima-8300). In order to measure the sample by XRF, 1 g powder of volcanic ash was added to a platinum crucible with 8 g of Lithium Borate (66.67% Li_2B4O_7, 32.83% $LiBO_2$, 0.5% LiBr) and mixed homogeneously. It was then transferred to the Fusion System for 20 min. For trace elements measurements done by ICP-OES (in ppm), the volcanic ash was crushed with HNO_3:165 $HClO_4$: HF (2.5:2.5:5 ml, v/v), doubly evaporated to incipient dryness with the addition 166 of HNO_3, and finally the volume was made up to 100 ml with 1.0% (v/v) HNO_3. The morphological analysis of raw and powder samples of volcanic ash was performed by scanning electron microscopy (SEM) (JEOL 7600) with a tungsten filament.

3. Results and discussion

The density measurement of samples was obtained by the Ultrapycnometer as shown in Table 1. The samples have bulk density range of 2.73–3.30 g/cc. Sample S7 has the lowest density (2.73 g/cc). This can be attributed directly to the molecular weight of chemical oxides in the XRF results shown in Table 2. The sample S7 has the lowest content of hematite (MW = 160 g/mol) and the highest alumina content (MW = 60 g/mol) as compared to other samples.

The XRD patterns of all samples show an existence of slight amorphous phase. This result can be referred to the nature of relatively rapid cooling of volcanic lavas. Fig. 2 shows the XRD of powder samples S3, S7, and S10. After identification of the powder data file, several minerals were found. In the sample S3, Albite (Na, Ca) $(Si,Al)_4O_8$ and hematite (Fe_2O_3) are major constituents while Augite is a minor component. Sample S7 contains mainly Quartz (SiO_2), and minor parts as Albite and Anorthoclase (Na,K)$(Si_3Al)O_8$. For sample S10, the identification shows Albite as a major portion and Anorthite as trace. However, the amorphous feature of silica present in the spectrum is considered as a main indication for the ceramic exploitation of volcanic ash as it is effective at low temperatures.

The chemical composition of all powder samples determined using XRF is expressed as wt% oxides and presented in Fig. 3. While, Table 3 gives the ICP-OES data for trace constituents (such as heavy metals and rare earth elements) of all the powdered samples. Fig. 3 shows that volcanic ash includes various quantities of silica (SiO_2), alumina (Al_2O_3), calcium oxide (CaO), and iron oxide (Fe_2O_3) as major elements; in addition to other minor oxides illustrated in the figure. The sample S7 has the highest percentage of SiO_2, as shown clearly in Fig. 3, and the lowest percentage of CaO, MgO, and Fe_2O_3. Based on the content of silica, it is obvious that the sample S7 is pumice, while other samples are scoria. Few and varying proportions of loss on ignition (L.O.I) remain in volcanic ash samples. The difference observed on (L.O.I) and the chemical composition of volcanic ashes is due to the historical conditions of volcanic eruption and volatile matter from the lower layers of Earth. Table 2 shows the comparison between the chemical composition of our volcanic ash sample and other volcanic ashes from the previous studies and suggested applications. In our samples, the results obtained showed that volcanic ash contains major elements including SiO_2 and Al_2O_3 that are around 44.8–71.6% and 10.8–16.64% respectively. The higher content of silica and alumina showed that volcanic ash could be used essentially for applications such as geopolymer synthesis. The classification depended on the amount and the silica to alumina molar ratio of amorphous phase (Djon Li Ndjock et al., 2017). The Hematite (Fe_2O_3) in our samples has potential applications in different areas like magnetic storage devices, catalysis, and sensors. The volcanic ash can also be used as an adsorbent by aluminol and silanol as the active adsorption sites (Kusmiyati et al., 2017). Our samples have quite high contained silica which allows us to use it in replacement of Portland cement, heat-insulating material, membrane filtration in wastewater and silica polymer network. Also, the amount of (K_2O + Na_2O + CaO) > 12 wt% indicates the possibility of their ceramic exploitation.

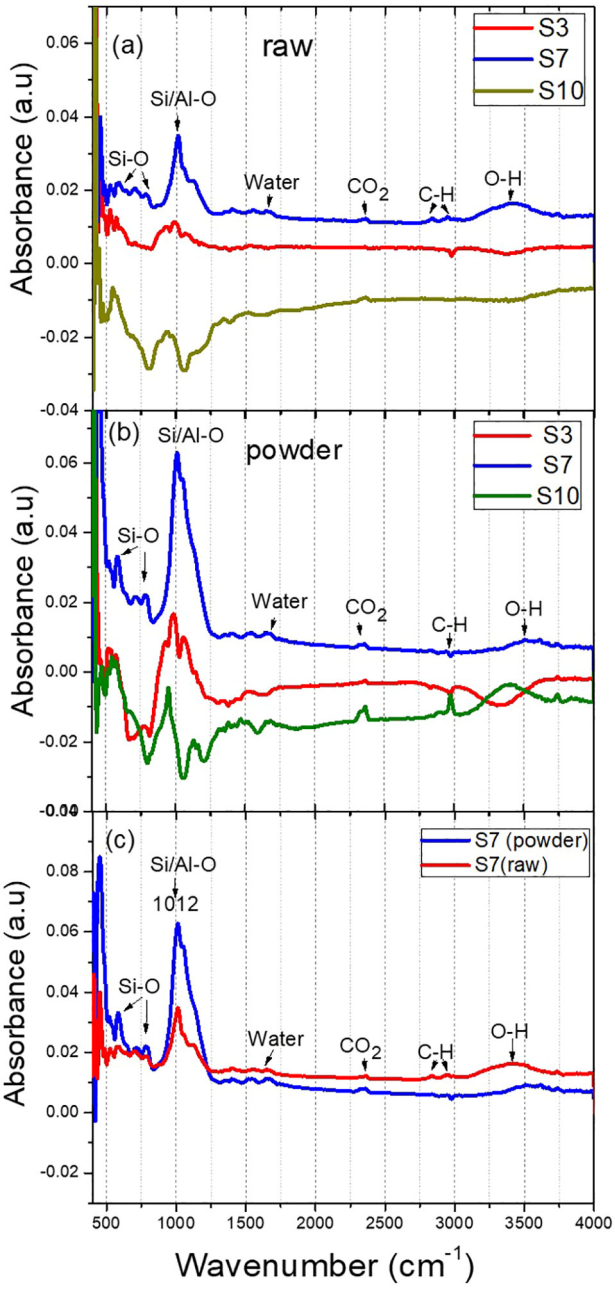

Fig. 4. FTIR spectra of: (a) raw volcanic ash samples S3, S7, and S10, (b) powder volcanic ash samples S3, S7, and S10, and (c) sample S7 in raw and powdered form.

As seen in Table 3, the volcanic ash contains trace elements including toxic substances and rare earth elements. The characteristics of the trace elements can provide valuable information related to the geochemistry of volcanic ash and the release of toxic elements into the environment that may have harmful impacts on the ecosystem and health. Some of these elements create more fertile soil and are beneficial to agriculture. Rare earth metals could be used in several areas such as memory storage, batteries, fluorescent lighting, and catalytic converters, while other trace elements

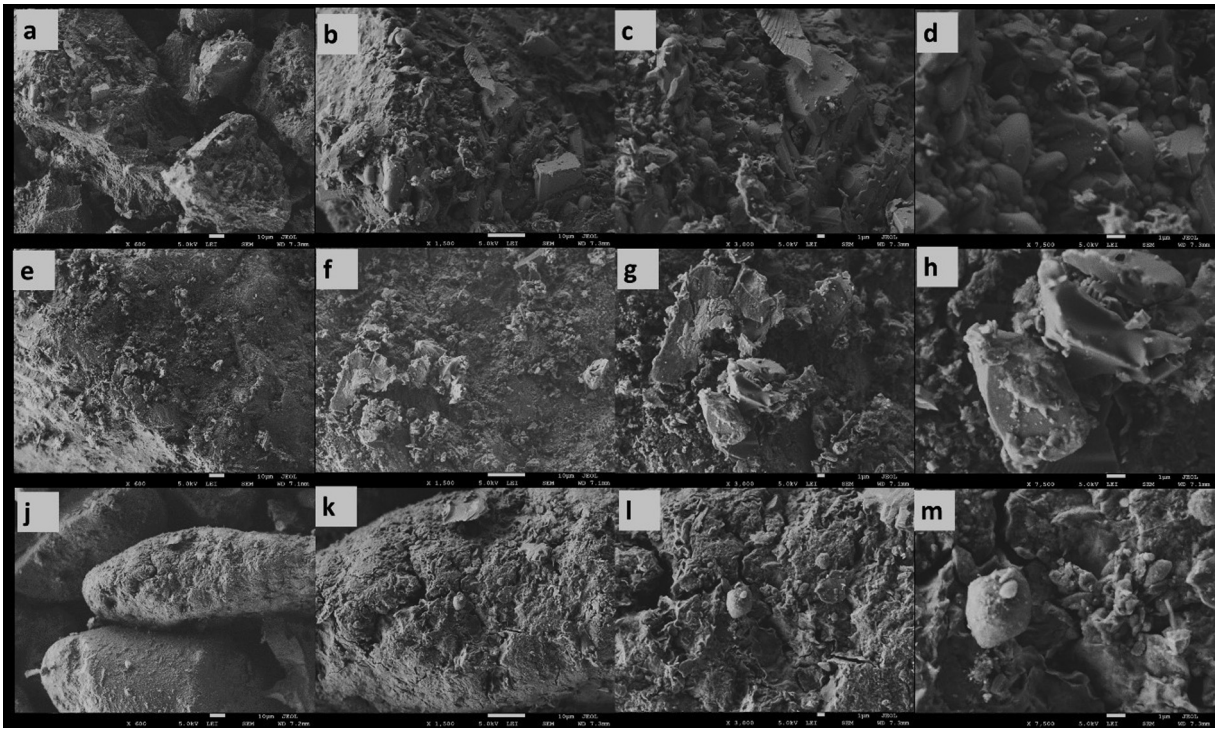

Fig. 5. SEM micrographs of raw volcanic ash samples S3 (a–d), S7 (e–h), and S10 (j–m) at different magnification.

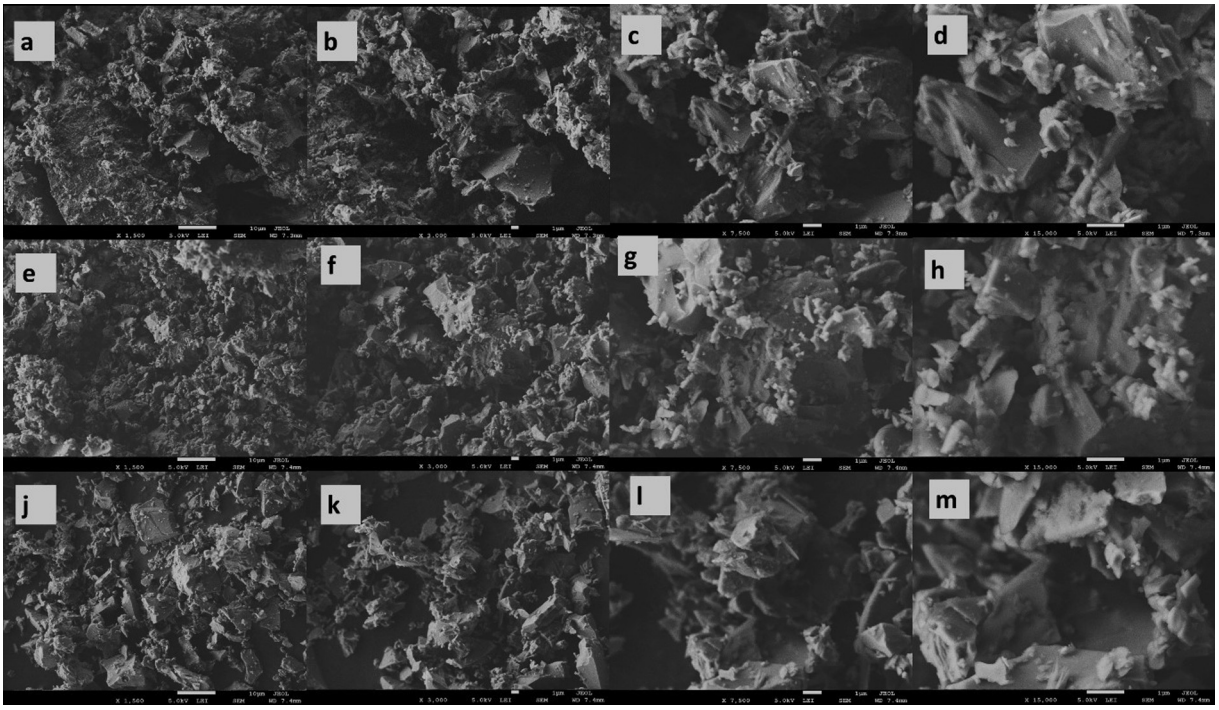

Fig. 6. SEM micrographs of powder volcanic ashes of samples S3 (a–d), S7 (e–h), and S10 (j–m) at different magnification.

could be potentially poisonous and could have negative effects on the environment (Ruggieri et al., 2012). The volcanic ash contains very low quantities of hazardous metals like: Silver (Ag), Arsenic (As), Cadmium (Cd), Chromium (Cr), and Lead (Pb) as shown in Table 3. We found that the values of As and Cd have lower range than Merapi volcanic ash were 8.948 and 1.30 mg/kg, respectively (Salamah and Wahyuni, 2018), the concentration of Molybdenum (Mo) is lower than Kelud volcanic ash were 31.4–42.7 mg/kg (Lestiani et al., 2018) and the values for Copper (Cu) were lower than in volcanic ashes from Copahue, Lonquimay, Llaima and Hudson in Chile and Argentina which varied from 41.05 to 108.70 mg/kg (Ruggieri et al., 2010). Maximum values of Cu, Co, Cr, Ni, and Sc

were observed in sample S6 while large concentrations of Zn, Mo, and Pb were observed in Samples 7, 15, and 14 respectively. These heavy metals are in similar concentrations for natural levels of heavy metals in soil (Tchounwou et al., 2012).

The FTIR spectra obtained for the raw and powder ash samples of S3, S7, and S10 are studied by a broad band as depicted in Fig. 4 (a–c). The bands between 500 and 900 cm^{-1} are attributed to the ring vibrations of Si–O bonds of the silicate group. The main band at about 1012 cm^{-1} is related to the stretching vibration of the Si–O–Al bond (Djobo et al., 2016; Huang, et al., 2016). The bands observed at 3420 and 1650 cm^{-1} correspond to the stretching and bending vibrations of O–H bonds from the silanol group and water molecules, respectively (Huang et al., 2016; Tchakouté et al., 2015). The bands at 2948–2833 cm^{-1} might be attributed to the C–H bond vibration of methane dissolved into the glassy phase, while the absorption band at about 2360 cm^{-1} indicate the presence of the CO_2 molecule (Fine and Stolper, 1986). The presence of CO_2, water, and methane is common in aluminosilicate glasses (Huang et al., 2016; Fine and Stolper, 1986). It is clearly shown in Fig. 5 that the intensity of Si-O bonds increases with decrease in the size of particles after grinding, in particular in Fig. 5c for sample S7 which is in agreement with XRD measurements. This result explains that after the grinding process the particle size decreases and the crystallinity changes.

Figs. 5 and 6 show the SEM analysis of the raw and powder samples at different magnification, respectively. Fig. 5(a–d) shows the SEM micrographs of S3 samples with poor red particles, classified as scoria type. Fig. 5(e–h) shows micrographs of S7 sample that has white particles, classified as pumice type. Fig. 6(j–m) micrographs of S10 sample that has dark particles, classified as scoria type. It is possible to notice from Fig. 5 that the microstructure and morphology of the raw ash samples S3, S7, and S10 were different. All raw volcanic ash samples have different angular particles with various particle sizes in the range from nano to microscale size. However, the shapes and sizes of the pumice particles were different from scoria particles. Moreover, the surface morphology of the pumice sample was characterized by smooth surfaces with high porosity more than scoria samples and that makes the pumice the lowest density. In general, all raw ash samples have irregular-shape morphology, non-uniform plate shape in addition to remnants of wall vesicle rupture. In Fig. 6, the SEM of powder volcanic ash of samples S3, S7 and S10 show a similar morphology of raw volcanic ash with sharp edges indicating that the grains suffered brittle fractures during the grounding processes. These results were expected because the volcanic ash samples are non-crystalline materials that confirmed using XRD analysis.

4. Conclusions

The crystalline phase, microstructure, chemical composition, and morphology of different powder volcanic ash samples were extensively investigated. The powder samples of volcanic ash demonstrated clear variations in mineralogical, elemental compositions, and morphology. The chemical composition analysis of volcanic ashes showed a wide spectrum of elements, with the major constituents being SiO_2, Al_2O_3, CaO, and Fe_2O_3; whereas, K_2O, MgO, MnO, Na_2O, P_2O_5, TiO_2, and SO_3 were the minor constituents. Further, the trace elements (As, Mo, Cd, Cr, Cu, Mn, and Pb) and rare earth elements were identified. These results can be used as a scientific database for achieving new desirable properties. In the future, the variety in mineralogy and chemical compositions of volcanic ash samples can open up an avenue for wider industrial applications. Moreover, environmental care and safety due to the presence of small quantities of hazardous trace elements must be given significant attention.

Disclosure of funding

Not applicable.

Declaration of Competing Interest

The authors declare that they have no known competing financial interests or personal relationships that could have appeared to influence the work reported in this paper.

Acknowledgements

The authors would like to acknowledge the technical support of the Center of Nanotechnology at King Abdul Aziz University, and Saudi Geological Survey.

References

Ahmaruzzaman, M., 2010. A review on the utilization of fly ash. Prog. Energy Combust. Sci., 36(3) 327–363. A review. Ceram. Int., 43(17), pp 14545–14551..
Alemayehu, E., Lennartz, B., 2009. Virgin volcanic rocks: kinetics and equilibrium studies for the adsorption of cadmium from water. J. Hazard. Mater. 169 (1–3), 395–401.
Alemayehu, E., Lennartz, B., 2010. Adsorptive removal of nickel from water using volcanic rocks. Appl. Geochem. 25 (10), 1596–1602.
Al-Fadala, S., Chakkamalayath, J., Al-Bahar, S., Al-Aibani, A., Ahmed, S., 2017. Significance of performance-based specifications in the qualification and characterization of blended cement using volcanic ash. Constr. Build. Mater. 144, 532–540.
Assaad, J.J., Nasr, D., Chwaifaty, S., Tawk, T., 2020. Parametric study on polymer-modified pigmented cementitious overlays for colored applications. J. Build. Eng. 27, pp101009.
Best, M.G., 2013. Igneous and metamorphic petrology. John Wiley & Sons.
Brown, R.J., Calder, E.S., 2005. Pyroclastics. Encycl. Geol., 386–397.
Cultrone, G., Sebastián, E., 2009. Fly ash addition in clayey materials to improve the quality of solid bricks. Constr. Build. Mater. 23 (2), 1178–1184.
Demirdag, S., Gunduz, L., 2008. Strength properties of volcanic slag aggregate lightweight concrete for high performance masonry units. Constr. Build. Mater. 22 (3), 135–142.
Djobo, J.N.Y., Elimbi, A., Tchakouté, H.K., Kumar, S., 2016. Reactivity of volcanic ash in alkaline medium, microstructural and strength characteristics of resulting geopolymers under different synthesis conditions. J Mater Sci 51 (22), 10301–10317.
Fine, G., Stolper, E., 1986. Dissolved carbon dioxide in basaltic glasses: concentrations and speciation. Earth Planet Sc Lett. 76 (3–4), 263–278.
Hossain, K.M.A., 2005. Volcanic ash and pumice as cement additives: pozzolanic, alkali-silica reaction and autoclave expansion characteristics. Cem. Concr. Res. 35 (6), 1141–1144.
Huang, Z., Wang, Z., Chen, F., Shen, Q., Zhang, L., 2016. Band structures and optical properties of Al-doped α-Si3N4: theoretical and experimental studies. Ceram Int. 42 (2), 3681–3686.
Kaid, N., Cyr, M., Julien, S., Khelafi, H., 2009. Durability of concrete containing a natural pozzolan as defined by a performance-based approach. Constr. Build. Mater. 23 (12), 3457–3467.
Kani, E.N., Allahverdi, A., Provis, J.L., 2012. Efflorescence control in geopolymer binders based on natural pozzolan. Cem. Concr. Comp. 34 (1), 25–33.
Koshino, M., 2001. Fertilizers with new functions. Environmental Conservation and Innovative Fertilization Technologies, p. 116..
Kumar, R., Kumar, S., Mehrotra, S.P., 2007. Towards sustainable solutions for fly ash through mechanical activation. Resour. Conserv. Recycl. 52 (2), 157–179.
Kusmiyati, K., Listiyanto, P.A., Vitasari, D., Indra, R., Islamica, D., Hadiyanto, H., 2017. Coal bottom ash and activated carbon for removal of vertigo blue dye in batik textile wastewater: adsorbent characteristic, isotherms, and kinetics studies. Walailak J. Sci. Technol. (WJST) 14 (5), 427–439.
Langmann, B., Zakšek, K., Hort, M., Duggen, S., 2010. Volcanic ash as fertiliser for the surface ocean. Atmos. Chem. Phys. 10 (8), 3891–3899.
Lemougna, P.N., MacKenzie, K.J., Melo, U.C., 2011. Synthesis and thermal properties of inorganic polymers (geopolymers) for structural and refractory applications from volcanic ash. Ceram. Int. 37 (8), 3011–3018.
Lemougna, P.N., Melo, U.C., Delplancke, M.P., Rahier, H., 2014. Influence of the chemical and mineralogical composition on the reactivity of volcanic ashes during alkali activation. Ceram. Int. 40 (1), 811–820.
Lemougna, P.N., Wang, K.T., Tang, Q., Nzeukou, A.N., Billong, N., Melo, U.C., Cui, X.M., 2018. Review on the use of volcanic ashes for engineering applications. Resour. Conserv. Recycl. 137, 177–190.
Lemougna, P.N., Nzeukou, A., Aziwo, B., Tchamba, A.B., Wang, K.T., Melo, U.C., Cui, X. M., 2020. Effect of slag on the improvement of setting time and compressive strength of low reactive volcanic ash geopolymers synthetized at room temperature. Mater. Chem. Phys. 239, 122077.

Leonelli, C., Kamseu, E., Boccaccini, D.N., Melo, U.C., Rizzuti, A., Billong, N., Miselli, P., 2007. Volcanic ash as alternative raw materials for traditional vitrified ceramic products. Adv. Appl. Ceram. 106 (3), 135–141.
Lestiani, D.D., Apryani, R., Lestari, L., Santoso, M., Hadisantoso, E.P., Kurniawati, S., 2018. Characteristics of trace elements in volcanic ash of Kelud eruption in East Java. Indones. J. Chem 18 (3), 457–463.
Liu, Y., Taylor, L.A., 2011. Characterization of lunar dust and a synopsis of available lunar simulants. Planetary Space Sci. 59 (14), 1769–1783.
Nakagawa, M., Ohba, T.S., 2002. Minerals in volcanic ash 1: Primary minerals and volcanic glass. Glob. Environ. Res. –Engl. Ed. 6 (2), 41–52.
Djon Li Ndjock, B.I., Elimbi, A., Cyr, M., 2017. Rational utilization of volcanic ashes based on factors affecting their alkaline activation. J Non-Cryst Solids 463, 31–39.
Ohba, T., Nakagawa, M., 2002. Minerals in volcanic ash 2: non-magmatic minerals. Glob Environ. Res.-Engl. Edit. 6 (2), 53–60.
Paulick, H., Franz, G., 1997. The color of pumice: case study on a trachytic fall deposit, Meidob volcanic field. Sudan. Bull. Volcanol. 59 (3), 171–185.
Querol, X., Umaña, J.C., Plana, F., Alastuey, A., Lopez-Soler, A., Medinaceli, A., Domingo, M.J., Garcia-Rojo, E., 2001. Synthesis of zeolites from fly ash at pilot plant scale. Examples of potential applications. Fuel 80 (6), 857–865.
Rocher, P., 1992. Mémento roches et minéraux industriels. Argiles nobles pour produits céramiques. Rapport BRGM 35743, 48.
Ruggieri, F., Fernandez-Turiel, J.L., Saavedra, J., Gimeno, D., Polanco, E., Amigo, A., Galindo, G., Caselli, A., 2012. Contribution of volcanic ashes to the regional geochemical balance: the 2008 eruption of Chaitén volcano, Southern Chile. Sci. Total Environ. 425, 75–88.
Ruggieri, F., Saavedra, J., Fernandez-Turiel, J.L., Gimeno, D., Garcia-Valles, M., 2010. Environmental geochemistry of ancient volcanic ashes. J. Hazard. Mater. 183 (1–3), 353–365.
Sabtan, A.A., Shehata, W.M., 2000. Evaluation of engineering properties of scoria in central Harrat Rahat, Saudi Arabia. Environ Geol. Eng. Bull. 59 (3), 219–225.
Salamah, S., Wahyuni, E.T., 2018. September. The characterization of Merapi volcanic ash as adsorbent for dyes removal from batik wastewater. IOP Conf. Ser. Mater. Sci. Eng. 403, (1) 012007.
Serra, M.F., Conconi, M.S., Suarez, G., Aglietti, E.F., Rendtorff, N.M., 2015. Volcanic ash as flux in clay based triaxial ceramic materials, effect of the firing temperature in phases and mechanical properties. Ceram. Int. 41 (5), 6169–6177.
Seyfi, S., Azadmehr, A.R., Gharabaghi, M., Maghsoudi, A., 2015. Usage of Iranian scoria for copper and cadmium removal from aqueous solutions. J. Cent. South. Univ. 22 (10), 3760–3769.
Siddique, R., 2011. Effect of volcanic ash on the properties of cement paste and mortar. Resour. Conserv. Recycl. 56 (1), 66–70.
Takeda, H., Hashimoto, S., Kanie, H., Honda, S., Iwamoto, Y., 2014. Fabrication and characterization of hardened bodies from Japanese volcanic ash using geopolymerization. Ceram. Int. 40 (3), 4071–4076.
Tchakoute, H.K., Elimbi, A., Yanne, E., Djangang, C.N., 2013. Utilization of volcanic ashes for the production of geopolymers cured at ambient temperature. Cem. Concr. Compos. 38, 75–81.
Tchakouté, H.K., Kong, S., Djobo, J.N.Y., Tchadjié, L.N., Njopwouo, D., 2015. A comparative study of two methods to produce geopolymer composites from volcanic scoria and the role of structural water contained in the volcanic scoria on its reactivity. Ceram. Int. 41 (10), 12568–12577.
Tchounwou, P.B., Yedjou, C.G., Patlolla, A.K., Sutton, D.J., 2012. Heavy metal toxicity and the environment. In: Molecular, Clinical and Environmental Toxicology. Springer, Basel, pp. 133–164.
Toniolo, N., Boccaccini, A.R., 2017. Fly ash-based geopolymers containing added silicate waste..
Wang, K.T., Lemougna, P.N., Tang, Q., Li, W., Cui, X.M., 2017. Lunar regolith can allow the synthesis of cement materials with near-zero water consumption. Gondwana Res. 44, 1–6.
Xu, G., Shi, X., 2018. Characteristics and applications of fly ash as a sustainable construction material: a state-of-the-art review. Resources. Conserv. Recycl. 136, 95–109.
Zhang, P., Huang, J., Shen, Z., Wang, X., Luo, F., Zhang, P., Wang, J., Miao, S., 2017. Fired hollow clay bricks manufactured from black cotton soils and natural pozzolans in Kenya. Constr. Build. Mater. 141, 435–441.
Zheng, Y., Wang, S., Ouyang, Z., Zou, Y., Liu, J., Li, C., Li, X., Feng, J., 2009. CAS-1 lunar soil simulant. Adv. Space Res. 43 (3), 448–454.
Zhuang, X.Y., Chen, L., Komarneni, S., Zhou, C.H., Tong, D.S., Yang, H.M., Yu, W.H., Wang, H., 2016. Fly ash-based geopolymer: clean production, properties and applications. J. Clean. Prod. 125, 253–267.